

Introduction to X-ray Magnetic Scattering

M. Altarelli

- 1. Why magnetic x-ray scattering? How?**
- 2. Non-Resonant and Resonant Scattering**
- 3. Examples with Hard and Soft X-rays**

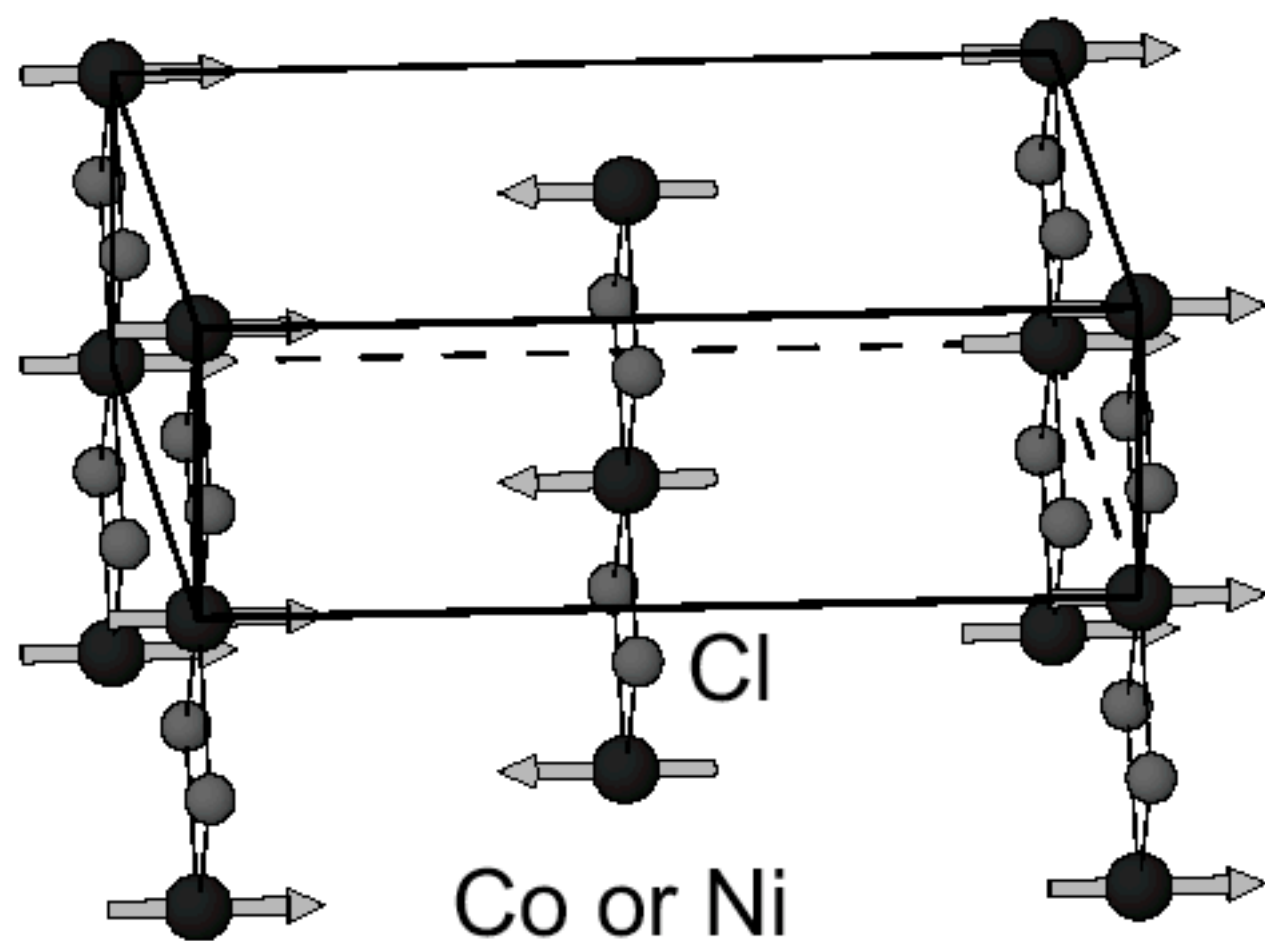


Fig. 4. Magnetic structure of $MCl_2(\text{bpy-d}8)$, $M = \text{Co}$ and Ni , below 5.0 or 8.5 K, respectively. The origin of the unit cell is shifted to $(\frac{1}{4}, \frac{1}{4}, 0)$. Only the metal and Cl atoms are shown

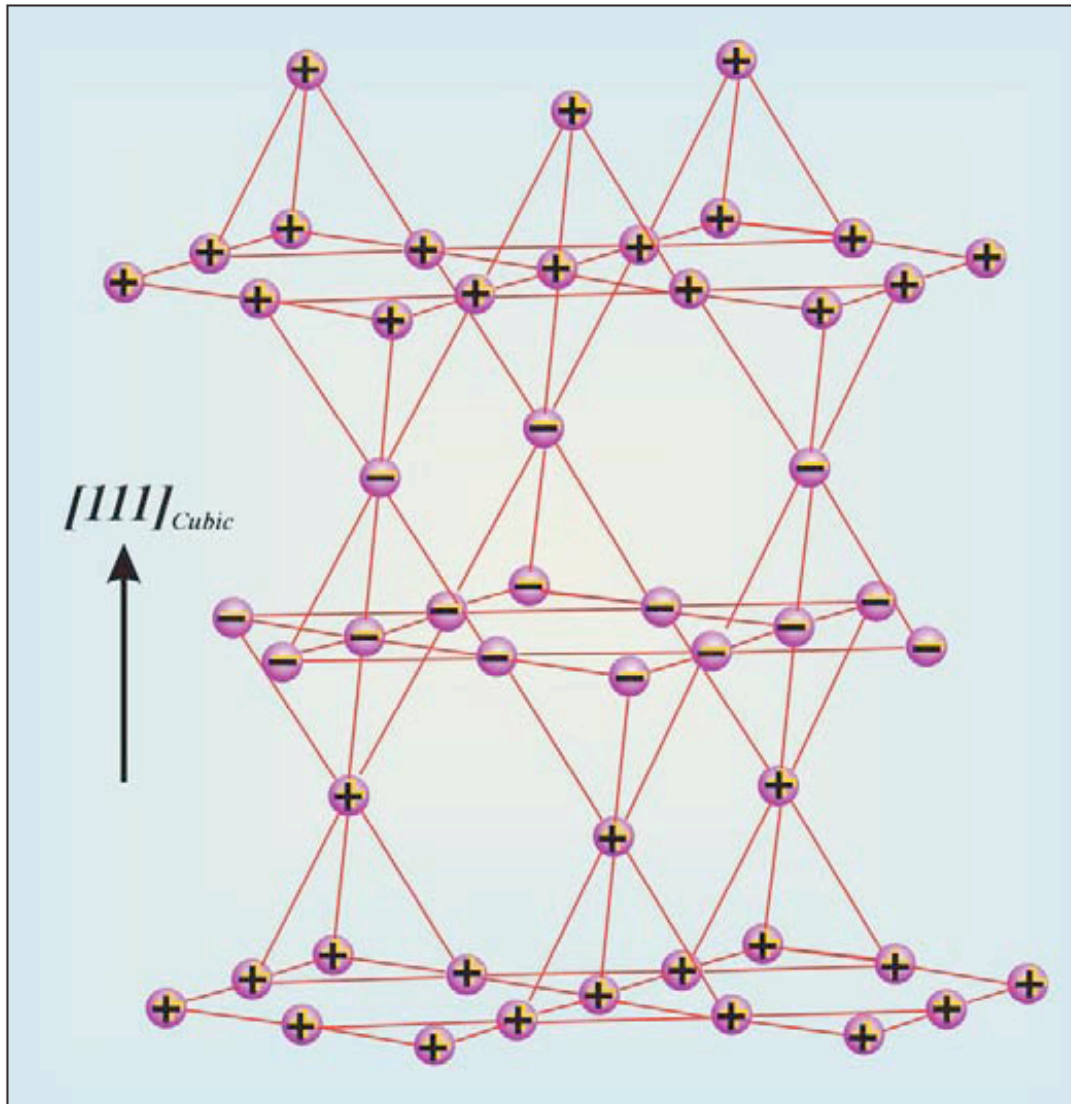
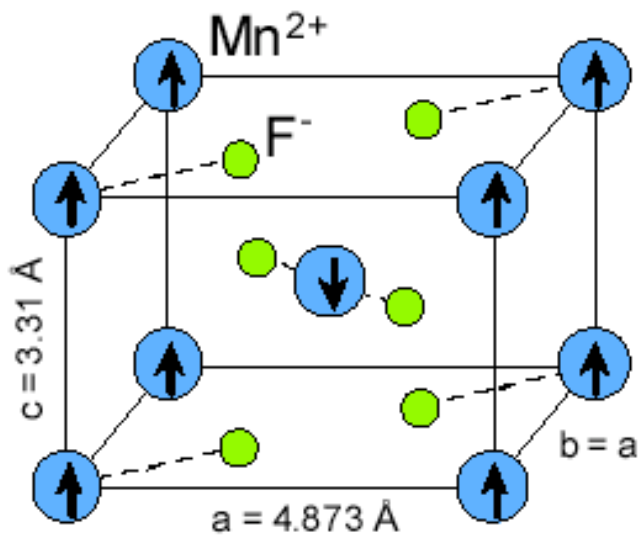
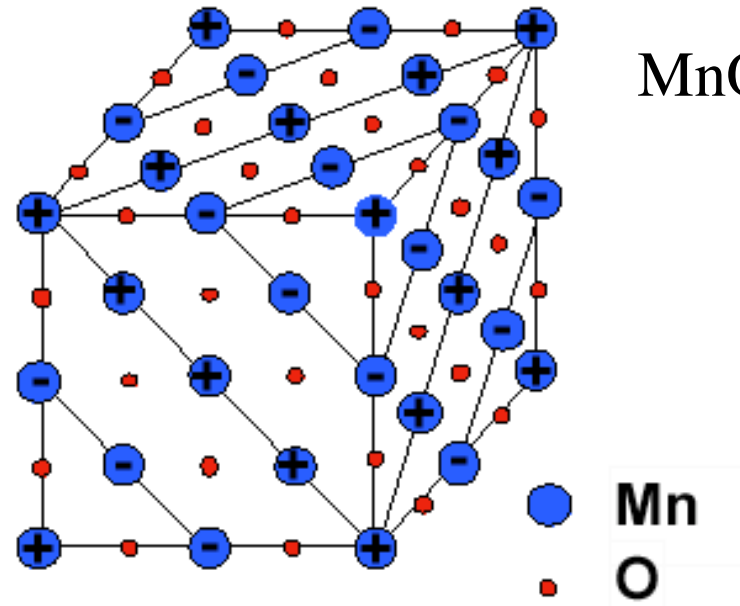


Fig. 1. A view of the crystal structure of GeNi_2O_4 , illustrating the magnetically frustrated corner-sharing tetrahedra. The relative Ni^{2+} spin directions are shown by the plus and minus signs for the two collinear magnetic sublattices.

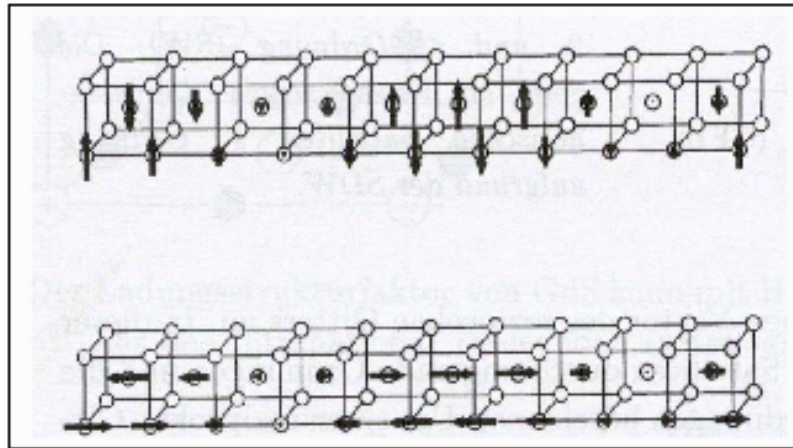
MnF₂



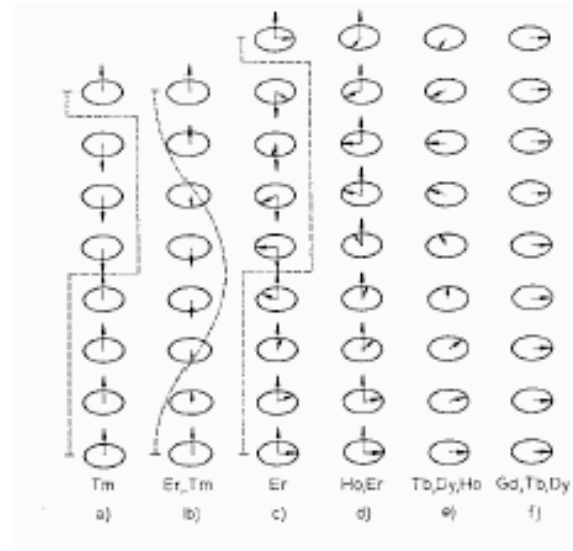
MnO



Cr



Rare
Earths



Determination of Magnetic Structures

NEUTRON SCATTERING is the standard probe for structure determination

X-RAY SCATTERING useful in special cases:

Small samples

High momentum space resolution (periods of incommensurate structures)

ORBITAL-SPIN separation (non-resonant)

Presence of more than one magnetic element (resonant)

Consider a system of electrons moving in the field of the nuclei, $V_N(\mathbf{r}_i)$ and interacting with one another via a Coulomb potential $V_c(|\mathbf{r}_i - \mathbf{r}_j|)$, described by the Hamiltonian:

$$\hat{H} = \sum_{ji} \frac{\vec{p}_i^2}{2m} + V_N(\vec{r}_i) + V_c(|\vec{r}_i - \vec{r}_j|) + (e\hbar / 2m^2 c^2) \vec{s}_i \cdot (\vec{E}(\vec{r}_i) \times \vec{p}_i)$$

The last term is the *Spin-Orbit* interaction.

Simplify this many-body Hamiltonian by somehow making an average potential for each electron:

$$\hat{H} = \sum_i \frac{\vec{p}_i^2}{2m} + V(\vec{r}_i) + (e\hbar / 2m^2 c^2) \vec{s}_i \cdot (\vec{E}(\vec{r}_i) \times \vec{p}_i)$$

Remember that every electron carries a spin 1/2 and a magnetic moment:

$$\vec{\mu}_i = (e\hbar / mc) \vec{s}_i$$

$$\mathbf{B} = \nabla \times \mathbf{A}$$

$$\mathbf{E} = -\nabla\Phi - (1/c)\frac{\partial\mathbf{A}}{\partial t},$$

Fields \mathbf{E} , \mathbf{B} from potentials A , Φ

where the vector $\nabla = \left(\frac{\partial}{\partial x}, \frac{\partial}{\partial y}, \frac{\partial}{\partial z}\right)$.

To describe electromagnetic waves, we can choose a gauge where the scalar potential $\Phi=0$, and the vector potential is:

$$\vec{A}(\vec{r}, t) = \sum_{k, \lambda} \left(\frac{he^2}{\Omega\omega_k}\right)^{1/2} [\vec{e}_\lambda a(\vec{k}, \lambda) e^{i(\vec{k} \cdot \vec{r} - \omega_k t)} + c.c.]$$

Normal.
Box Volume

Polarization
vector $\lambda=1,2$

$\omega_k = ck$

General recipe (from classical physics) to introduce interaction of electrons with field $\mathbf{A}(\mathbf{r},t)$: $\mathbf{p} \Rightarrow \mathbf{p} - (e/c)\mathbf{A}$.
 Also: do not forget interaction of magnetic moment \mathbf{m} with magnetic field of radiation:

Kinetic Energy

$\mu \cdot \mathbf{B}$

$$\hat{H} = \sum_{i=1,N} \left[\frac{(\vec{p}_i - (e/c)\vec{A}(\vec{r}_i))^2}{2m} + V(\vec{r}_i) - (e\hbar/mc)\vec{s}_i \cdot \vec{B} - (e\hbar/2m^2c^2)\vec{s}_i \cdot (\vec{E} \times (\vec{p}_i - (e/c)\vec{A}(\vec{r}_i))) \right]$$

Spin-Orbit

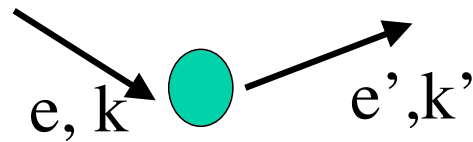
$$H_{int} = \sum_{i=1}^N \left[\boxed{H_1} - (e/mc) \mathbf{A}(\mathbf{r}_i) \cdot \mathbf{p}_i - \boxed{H_2} \right]$$

$$\boxed{H_3} + (e\hbar/mc) \mathbf{s}_i \cdot (\nabla \times \mathbf{A}(\mathbf{r}_i)) +$$

$$\boxed{H_4} (e\hbar/2m^2c^3) \mathbf{s}_i \cdot [(\partial \mathbf{A}(\mathbf{r}_i)/\partial t) \times (\mathbf{p}_i - (e/c) \mathbf{A}(\mathbf{r}_i))]$$

We already encountered H_1 and H_2 . There are two new terms, H_3 and H_4 , that are related to the *electron spin*

Elastic Scattering Processes



This photon present
in the initial state

$$|i\rangle = |0; \dots, (\mathbf{e}_\lambda, \mathbf{k}), \dots\rangle;$$

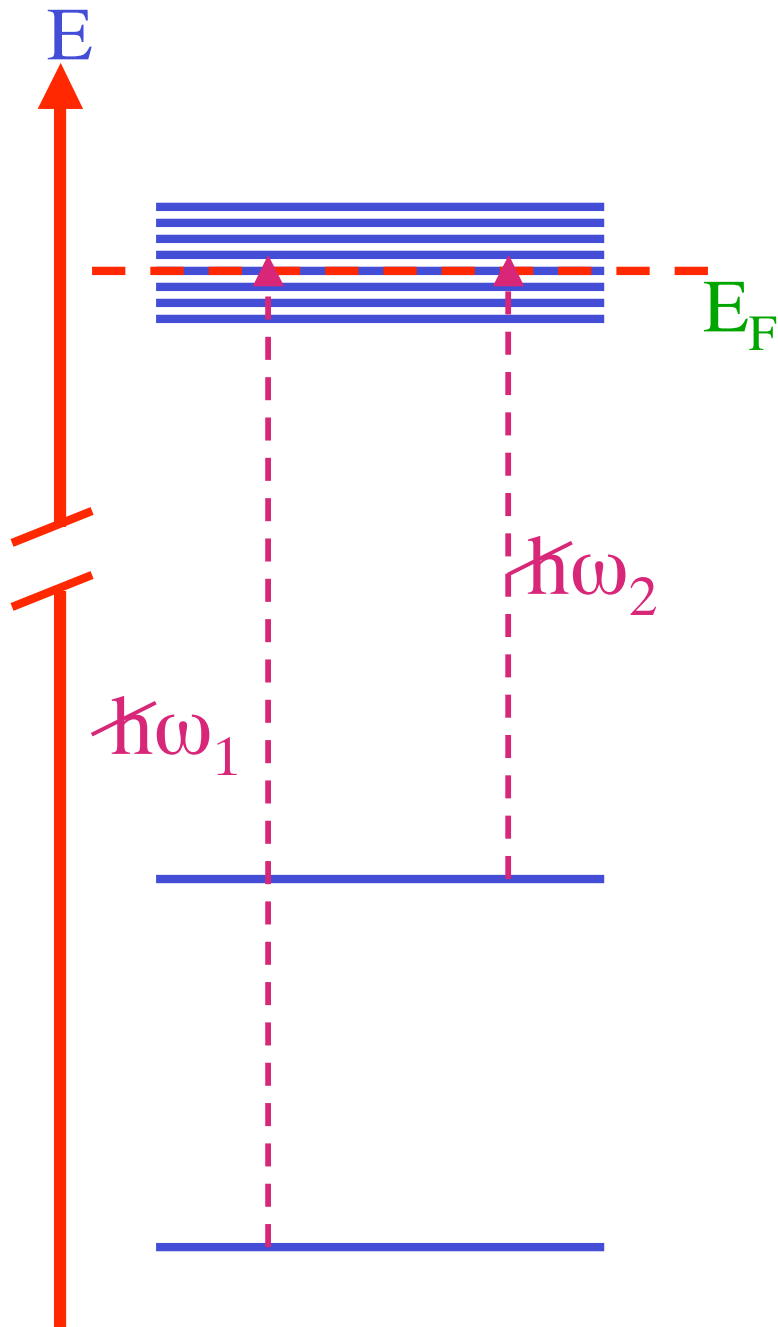
$$|f\rangle = |0; \dots, (\mathbf{e}'_{\lambda'}, \mathbf{k}'), \dots\rangle$$

Electronic
ground state

This photon present
in the final state

We saw in a previous lecture how H_1 gives origin to **Thompson scattering**. Including the three other pieces gives additional terms that can be derived in detail.

Before describing them we must discuss the difference between **non-resonant** and **resonant** scattering.



A

Non-resonant:
 $\hbar\omega \gg \hbar\omega_1, \hbar\omega_2$

B

Resonant:
 $\hbar\omega \cong \hbar\omega_1$
 OR
 $\hbar\omega \cong \hbar\omega_2$

A

In the non-resonant case $(\hbar\omega \gg \hbar\omega_1, \hbar\omega_2)$

all of the 4 terms contribute

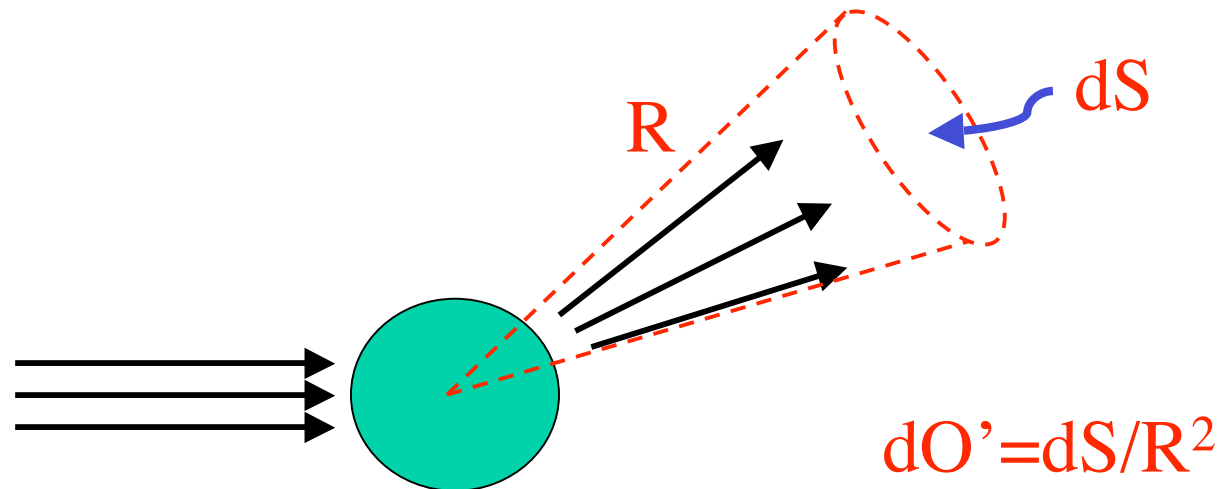
B

In the resonant case $(\hbar\omega \cong \hbar\omega_1 \text{ or } \hbar\omega \cong \hbar\omega_2)$

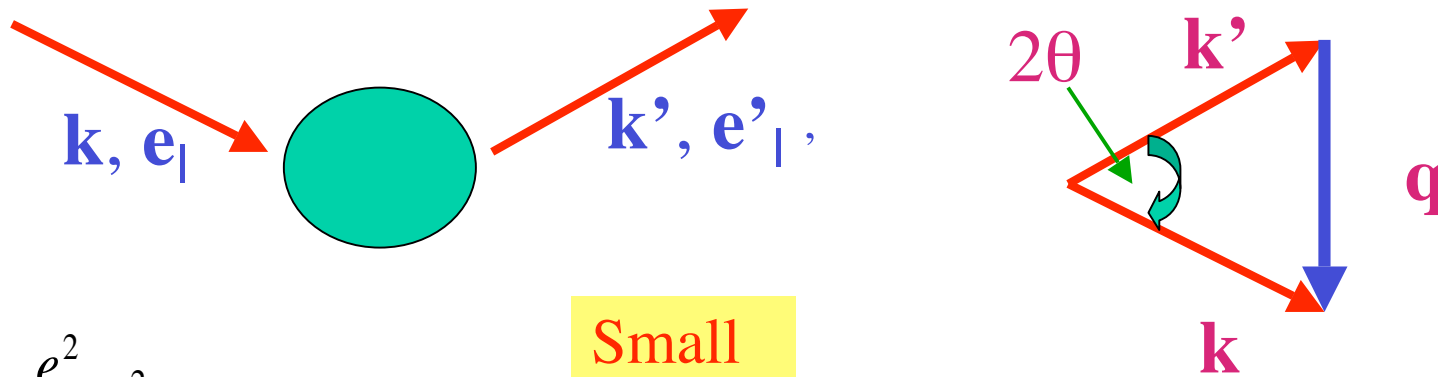
the term $H_2 = (e/mc) \Sigma \mathbf{A}(\mathbf{r}_i) \cdot \mathbf{p}_i$ dominates all others

The quantity that best describes the intensity of the elastic scattering is the differential cross section:

$$\frac{d\sigma}{d\Omega'} = \frac{\text{Number of photons per unit time scattered within } d\Omega'}{\text{Number of incident photons per unit time per unit surface}}$$



A Non-resonant scattering



$$\frac{d\sigma}{d\Omega} = \left(\frac{e^2}{mc^2}\right)^2 \cdot$$

Small factor!

$$\left| \sum_j \langle 0 | e^{i\vec{q}\cdot\vec{r}_j} | 0 \rangle (\vec{e}'^*_{\lambda'} \cdot \vec{e}_\lambda) - i \frac{\hbar\omega_{\vec{k}}}{mc^2} \left[\frac{mc}{e\hbar} \langle 0 | \hat{q} \times [\vec{M}_L(\vec{q}) \times \hat{q}] | 0 \rangle \cdot \vec{P}_L + \frac{mc}{e\hbar} \langle 0 | \vec{M}_S(\vec{q}) | 0 \rangle \cdot \vec{P}_S \right] \right|^2$$

Thompson
(charge scattering)

F.T. of *orbital*
moment density

F.T. of *spin*
moment density

90° dephasing

A Non-resonant scattering

Definitions:

$$\hat{q} = \frac{\vec{q}}{q}$$

$$\vec{M}_L(\vec{q}) = \sum_i e^{i\vec{q}\cdot\vec{r}_i} \vec{M}_L(\vec{r}_i)$$

$$\vec{M}_S(\vec{q}) = \sum_i e^{i\vec{q}\cdot\vec{r}_i} \vec{s}_i$$

$$\vec{P}_L = (\vec{e}' *_{\lambda'} \times \vec{e}_\lambda) 4 \sin^2 \theta$$

$$\vec{P}_S = [(\vec{k}' \times \vec{e}' *_{\lambda'}) (\vec{k}' \cdot \vec{e}_\lambda) - (\vec{k} \times \vec{e}_\lambda) (\vec{k} \cdot \vec{e}' *_{\lambda'}) - (\vec{k}' \times \vec{e}' *_{\lambda'}) \times (\vec{k} \times \vec{e}_\lambda)]$$

A Non-resonant scattering

1. Is very weak compared to Thompson scattering

$$\left(\frac{\hbar\omega}{mc^2}\right)^2 \cong \left(\frac{10keV}{511keV}\right)^2 \cong \frac{1}{2500}$$
$$N_{mag} < Z$$

2. Has a very different polarization factor for orbital M_L and spin M_S components of the magnetic moment. Therefore selecting the incoming photon polarization and analyzing the outgoing photon polarization one can see either “orbital” or “spin” scattering

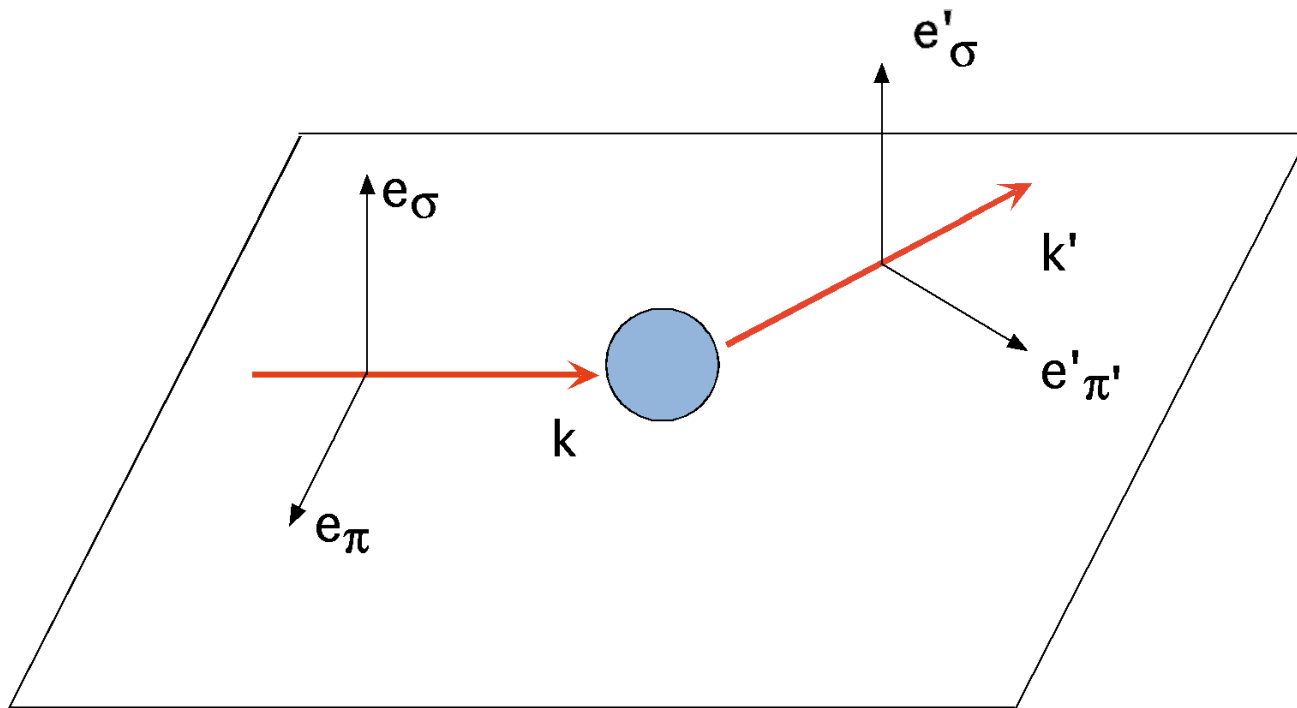


Fig. 1a

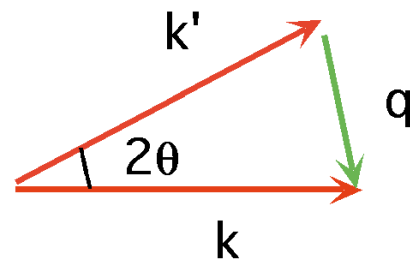
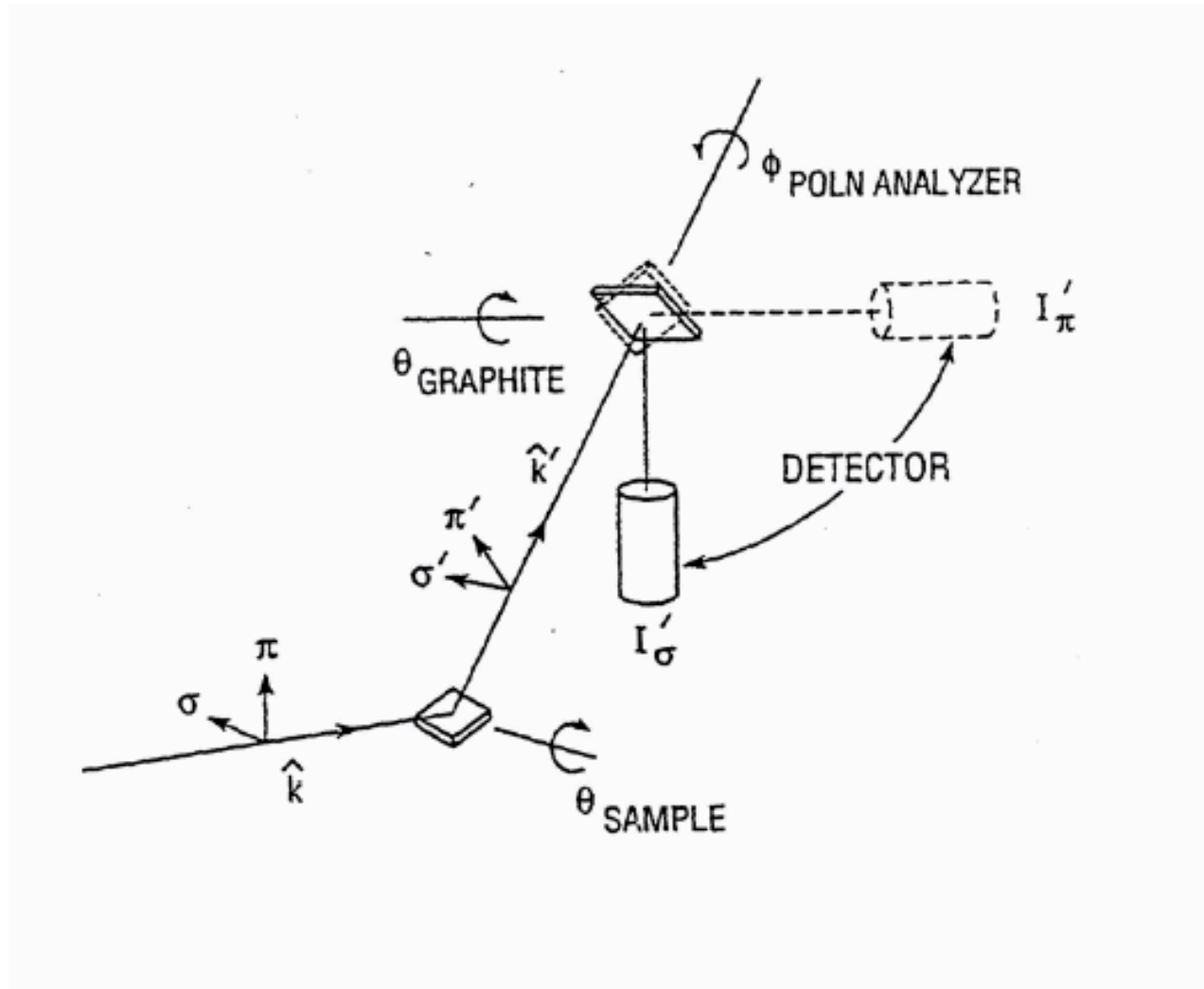
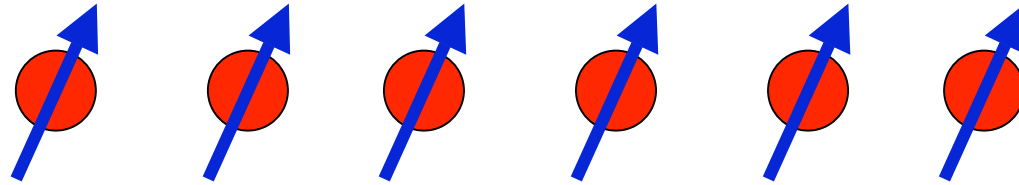


Fig. 1b



Analysis of polarization by 90° scattering on a “poor” crystal

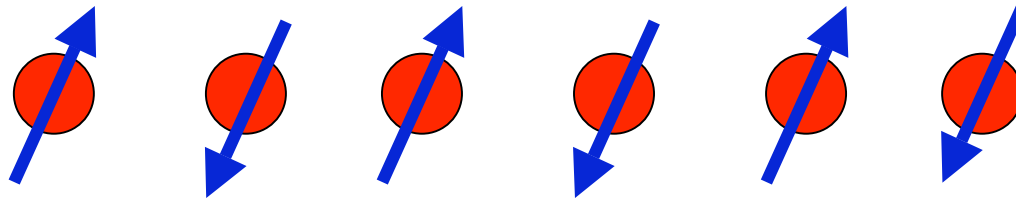
Observation of Magnetic X-ray Scattering



Ferromagnet : magnetic periodicity=lattice periodicity



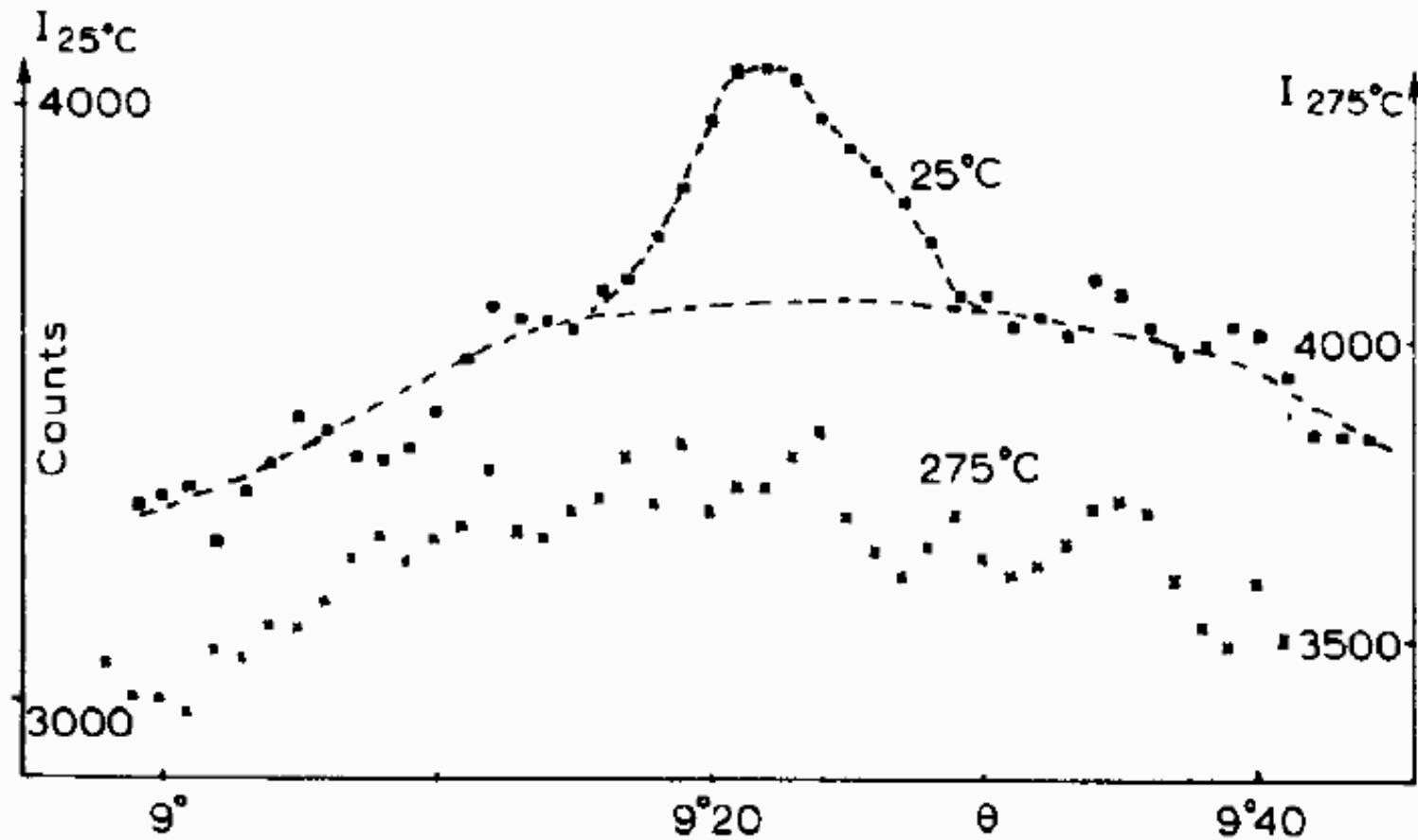
Same reciprocal lattice vectors



Antiferromagnet : magnetic periodicity= multiple of lattice periodicity



Additional magnetic reciprocal lattice vectors

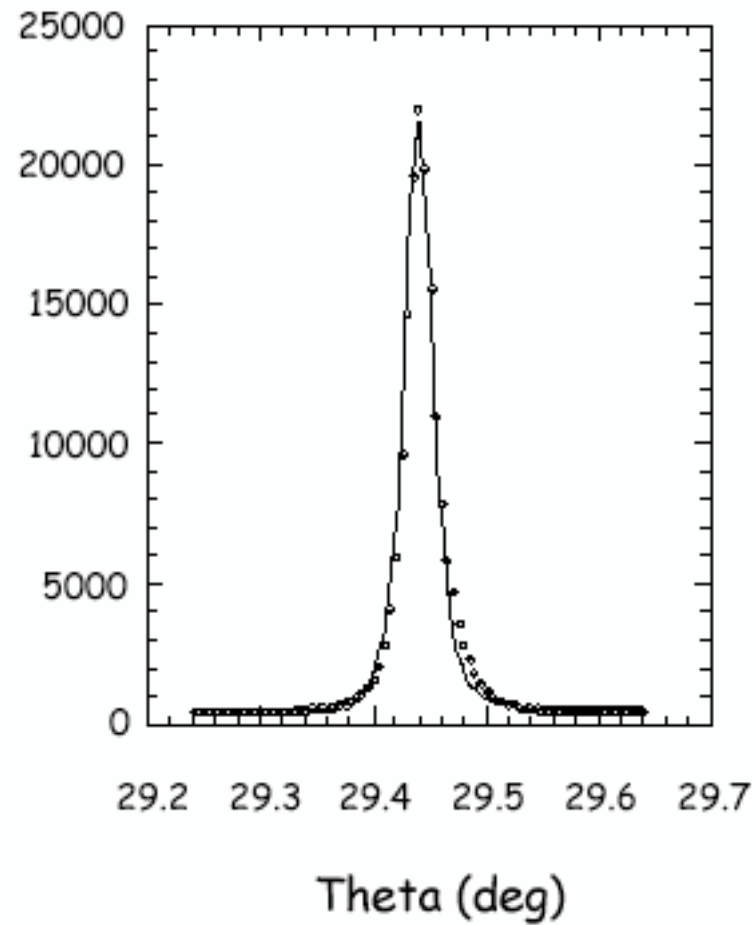


De Bergevin & Brunel, Phys. Lett. **A39**, 141 (1972)

Laboratory x-ray tube

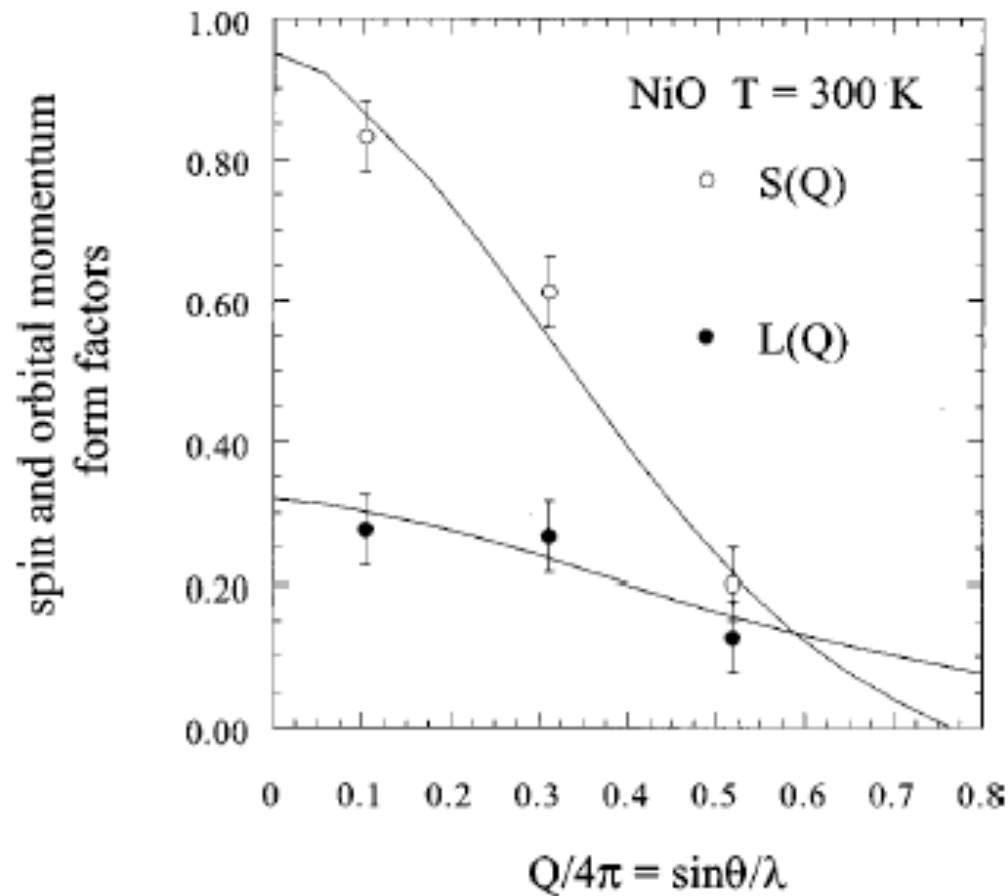
NiO ($3/2; 3/2; 3/2$) reflection, counts /225 minutes

NiO T=300 K (3/2 3/2 3/2)



ESRF ID20 Beamline (counts/s)

V. Fernandez *et al.*, *Phys Rev.* **B57**, 7870 (1998)



V. Fernandez *et al.*,
Phys Rev. B **57**, 7870 (1998)

FIG. 6. Spin form factor and orbital-moment form factor in NiO. The data have been obtained by normalizing magnetic intensities to charge peaks corrected for extinction. Extrapolations at $K = 0$ provide a value for the thermal average of $S = 0.95 \pm 0.10$ and $L = 0.32 \pm 0.05$ which lead to a value of $2.2 \pm 0.3 \mu_B$ for the staggered magnetization at $T = 300$ K. The continuous lines are the calculated variations of $S(\mathbf{Q})$ and $L(\mathbf{Q})$ with $\sin \theta/\lambda$ from Refs. 18 and 24 with an expansion of the \mathbf{Q} scale by 17%.

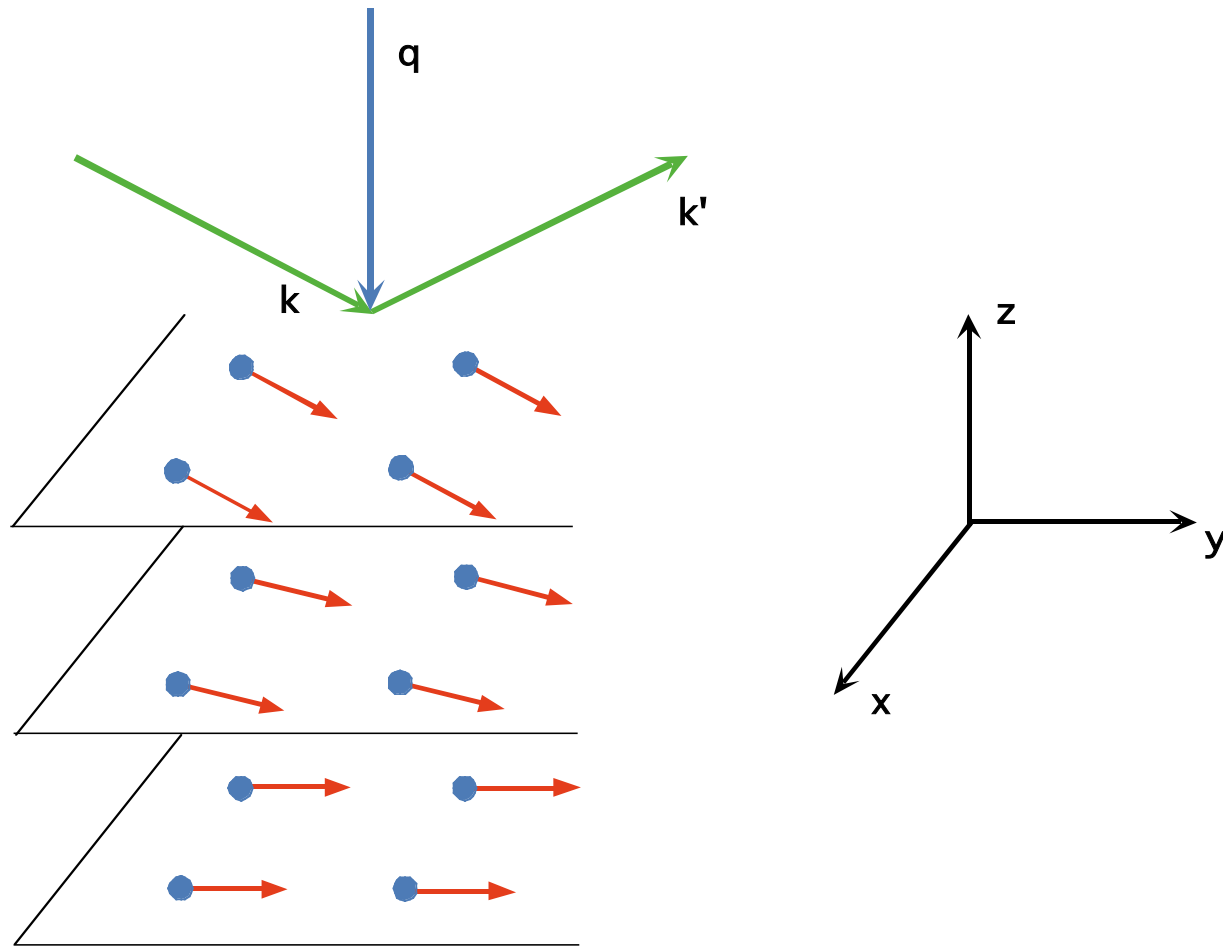


Fig. 6 Sketch of a basal-plane spiral antiferromagnet, and the scattering geometry

Arrangement of Moments in Holmium

Magnetic X-Ray Scattering Studies of Holmium Using Synchrotron Radiation

Doon Gibbs, D. E. Moncton, K. L. D'Amico, J. Bohr,^(a) and B. H. Grier^(b)

Department of Physics, Brookhaven National Laboratory, Upton, New York 11973

(Received 26 March 1985)

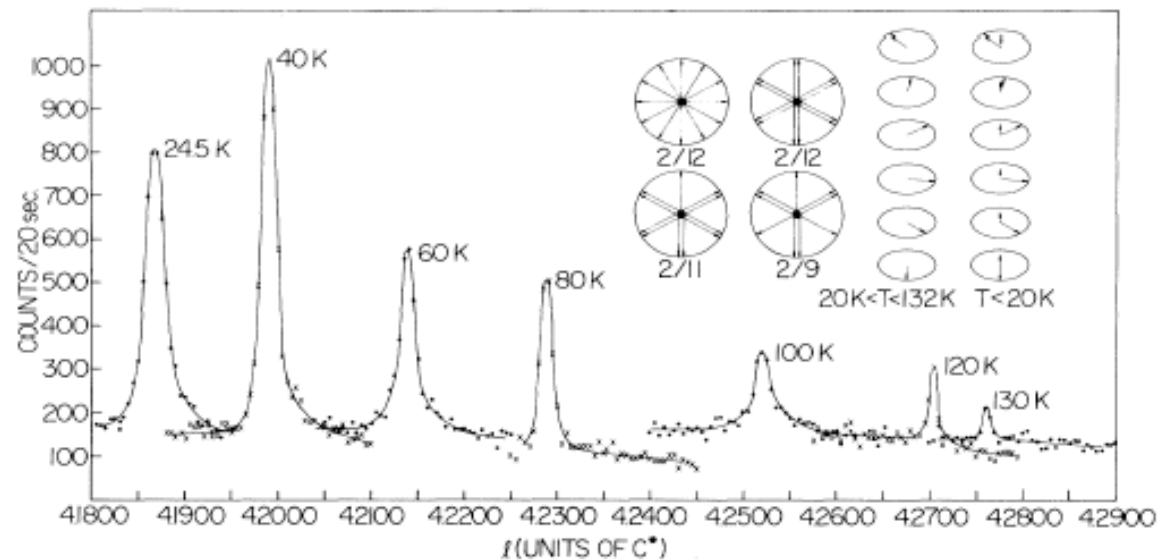
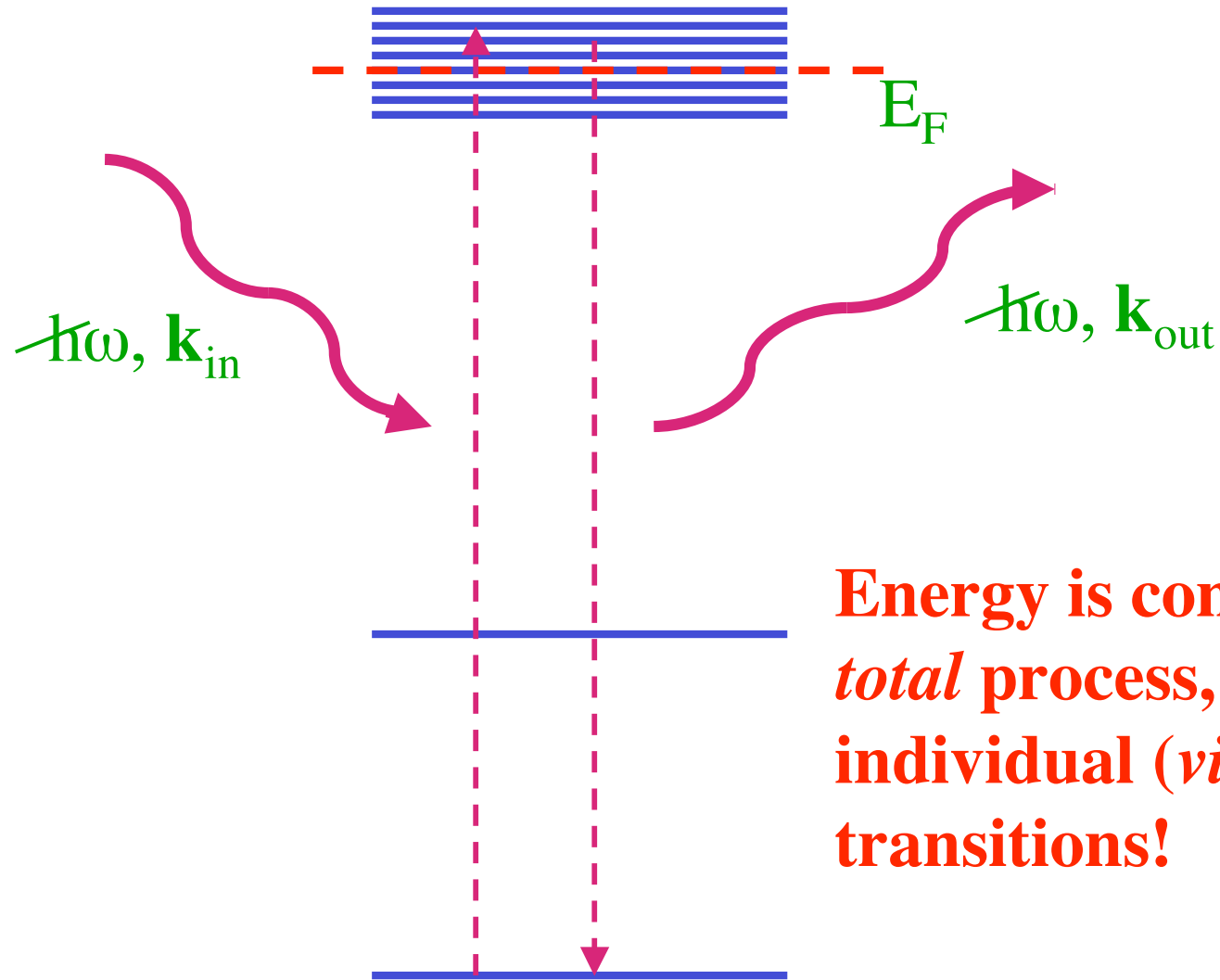


FIG. 1. Temperature dependence of the $\text{Ho}(004)^+$ magnetic satellite taken with synchrotron radiation (lines drawn to guide the eye). Inset: Right, schematic representation of the magnetic structure of Ho (after Koehler⁹). Left, projections of the magnetic unit cell for different spin-slip structures. For simplicity the doublet has been drawn as two parallel spins.

Synchrotron X-rays have excellent angular resolution!

B Resonant (Anomalous) Scattering



Energy is conserved in the *total* process, not in the individual (*virtual*) transitions!

B Resonant scattering

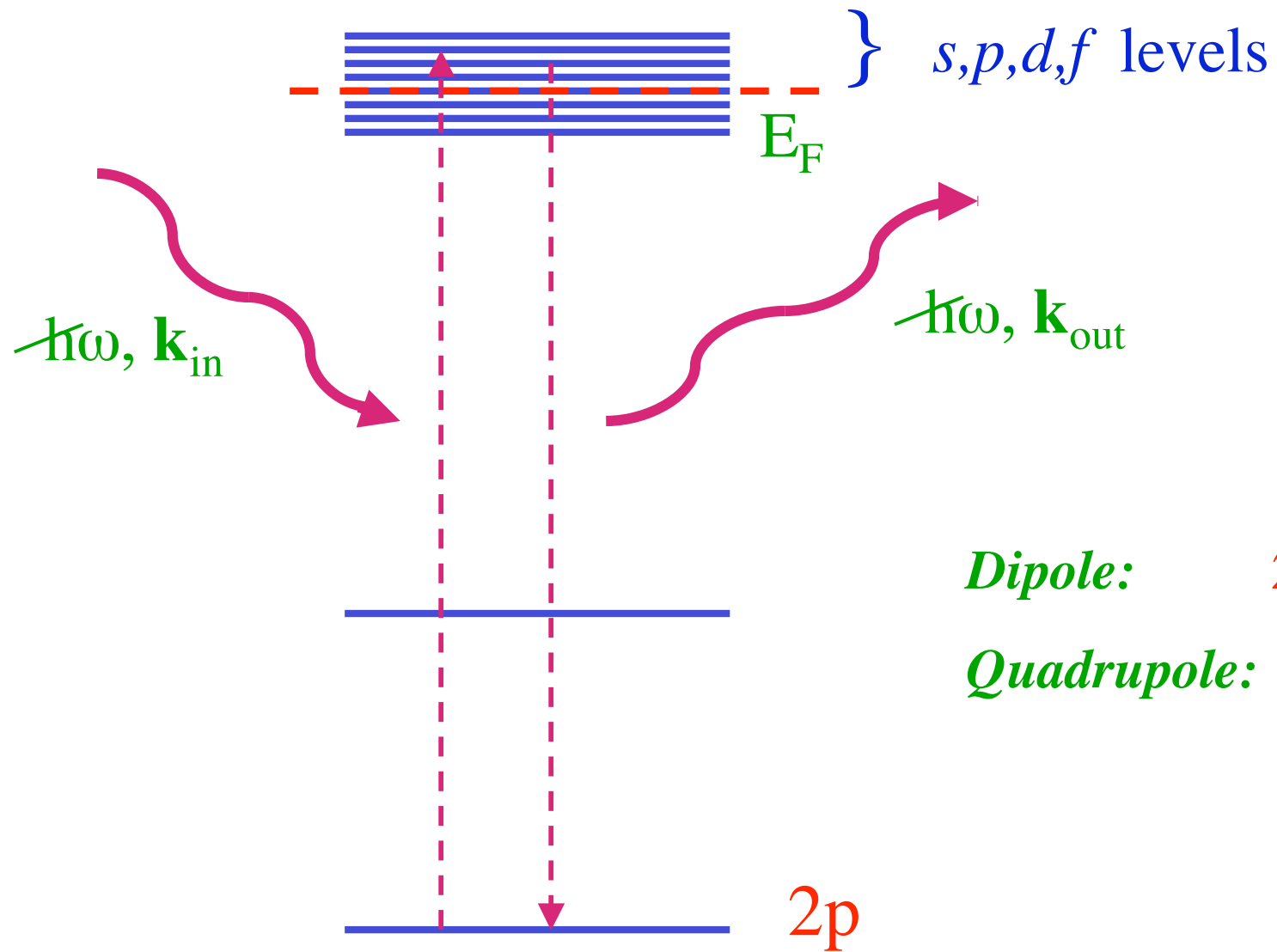
Differential
cross section

$$\frac{d\sigma}{d\Omega'} = |f_{res}|^2$$

Scattering amplitude

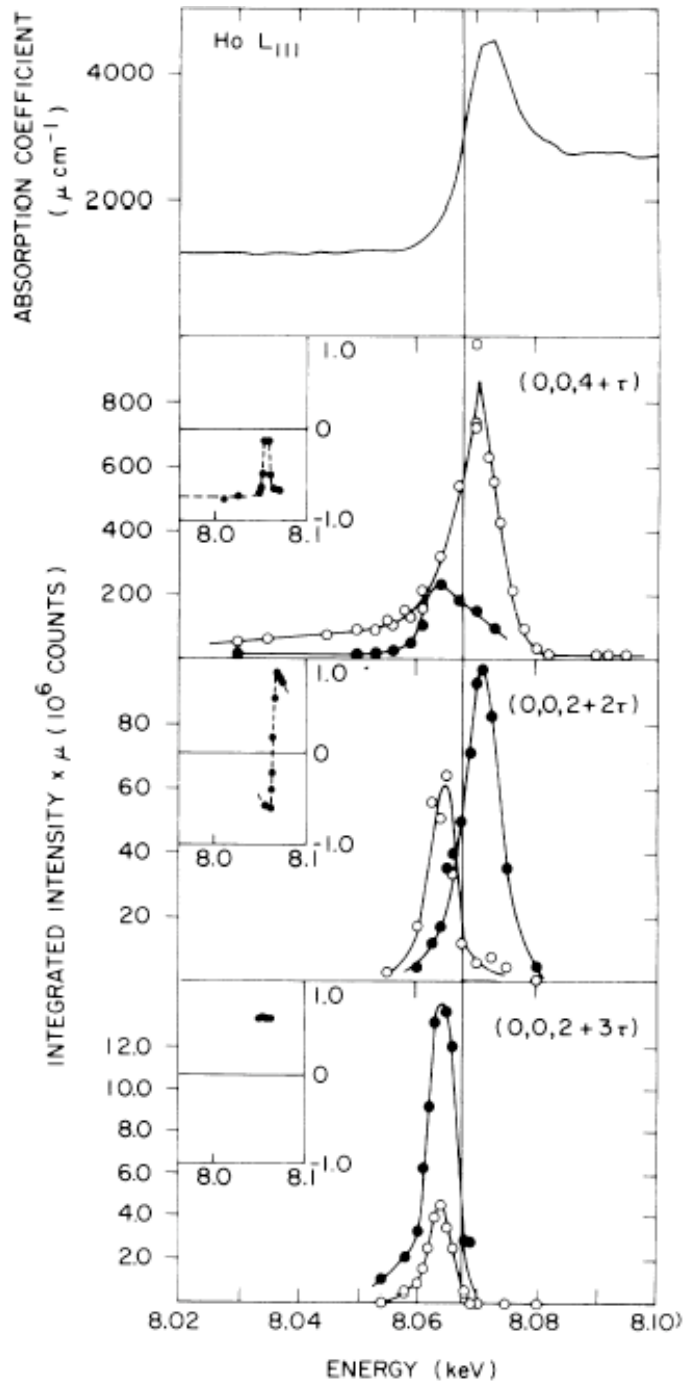
$$f_{res} \cong \sum_n \frac{\langle 0 | \hat{\varepsilon}^* \cdot \vec{p} e^{i\vec{k} \cdot \vec{r}} | n \rangle \langle n | \hat{\varepsilon}' \cdot \vec{p} e^{-i\vec{k}' \cdot \vec{r}} | 0 \rangle}{E_n - E_0 - \hbar\omega + i\Gamma_n / 2}$$

Multipole expansion: $e^{i\vec{k} \cdot \vec{r}} \cong 1 + i\vec{k} \cdot \vec{r} + \dots$



Dipole: $2p \rightarrow s, d$

Quadrupole: $2p \rightarrow f$



D. Gibbs et al.,

Phys. Rev. Lett. **61**, 1241(1988)

Holmium, L_3 ($2p_{3/2}$ edge)

Polarization:

- **Parallel to scatt. Plane**
- **Perpendicular to scatt. plane**

B Resonant Magnetic Scattering

1. Is very intense (10^2 - 10^4 times more than non-resonant)

2. Is element specific (via the core level binding energy)

3. Its intensity is less directly related to magnetic moments

Hannon-Trammell formula for dipole-dipole scattering

Definitions: $\vec{R} \equiv (X, Y, Z) = \sum_j \vec{r}_j$

$$R_0 = iZ, R_{\pm 1} = \mp(i/\sqrt{2})(X \pm iY)$$

\hat{z} Unit vector in z direction

$$f_{res} = -\frac{e^2}{mc^2} \left[\frac{1}{2} (\vec{e}'^*_{\lambda'} \cdot \vec{e}_{\lambda}) (F_{1,1}^{(e)} + F_{1,-1}^{(e)}) \right. \\ \left. - \frac{i}{2} (\vec{e}'^*_{\lambda'} \times \vec{e}_{\lambda}) \cdot \hat{z} (F_{1,1}^{(e)} - F_{1,-1}^{(e)}) \right. \\ \left. + (\vec{e}'^*_{\lambda'} \cdot \hat{z}) (\vec{e}_{\lambda} \cdot \hat{z}) (F_{1,0}^{(e)} - F_{1,1}^{(e)} - F_{1,-1}^{(e)}) \right]$$

Hannon *et al.*, Phys. Rev. Lett. 61, 1245 (1988)

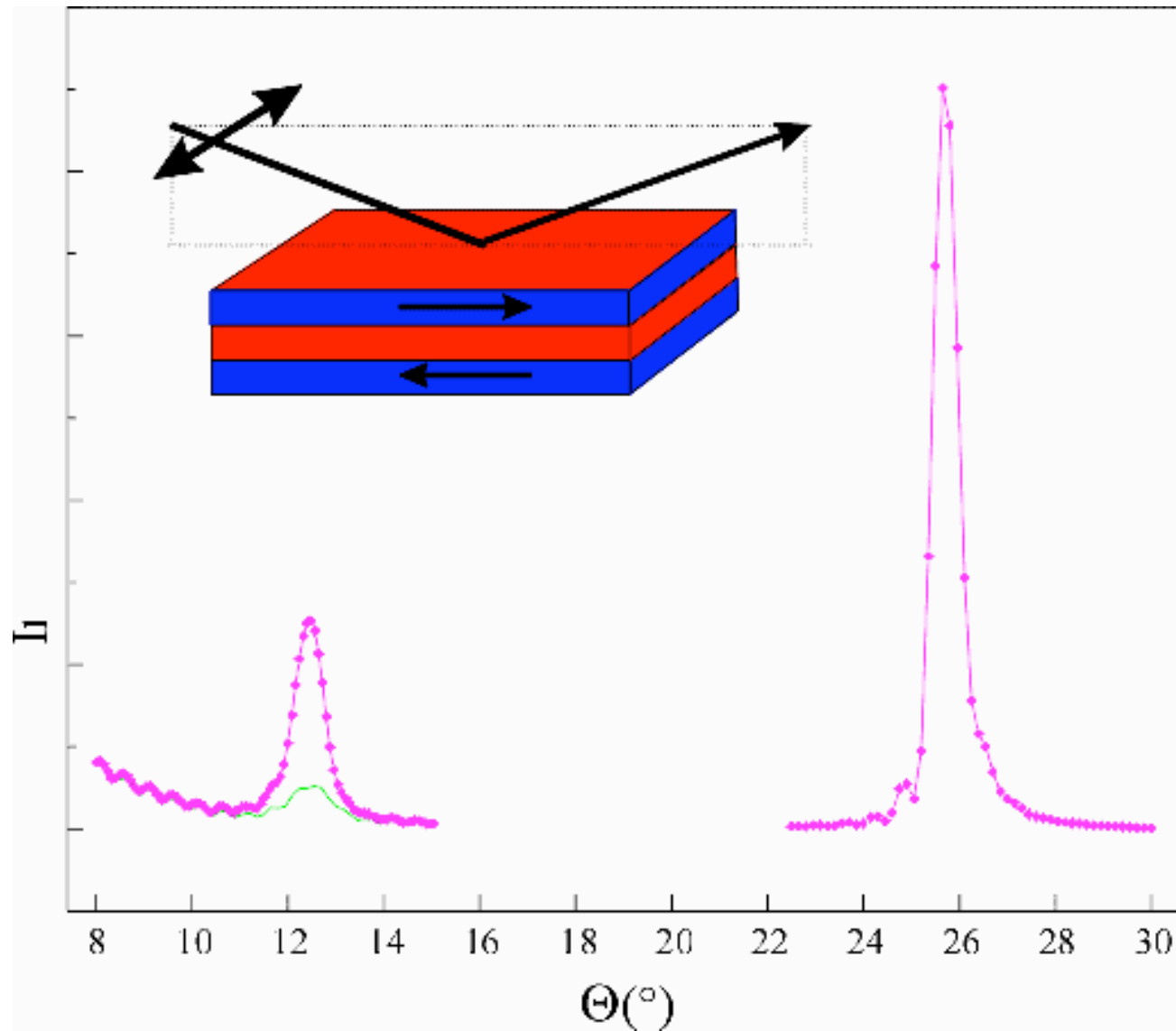
Soft X-ray Magnetic scattering:
structures with long periods.

Artificial structures (multilayers)

Complex compounds with large
structural and/or magnetic unit cells

$L_{2,3}$ edges of 3d transition metals

$2p \rightarrow 3d$



H Dürr *et al.*, $[\text{Co}(1 \text{ nm}) \text{Cu}(1 \text{ nm})]_{50}$ multilayer, Co L_3 -edge ($\sim 778 \text{ eV}$)

Soft X-Ray Resonant Magnetic Diffraction

S. B. Wilkins* and P. D. Hatton†

Department of Physics, University of Durham, Rochester Building, South Road, Durham DH1 3LE, United Kingdom

M. D. Roper

CLRC, Daresbury Laboratory, Warrington, Cheshire WA4 4AD, United Kingdom

D. Prabhakaran and A. T. Boothroyd

Department of Physics, University of Oxford, Clarendon Laboratory, Parks Road, Oxford OX1 3PU, United Kingdom

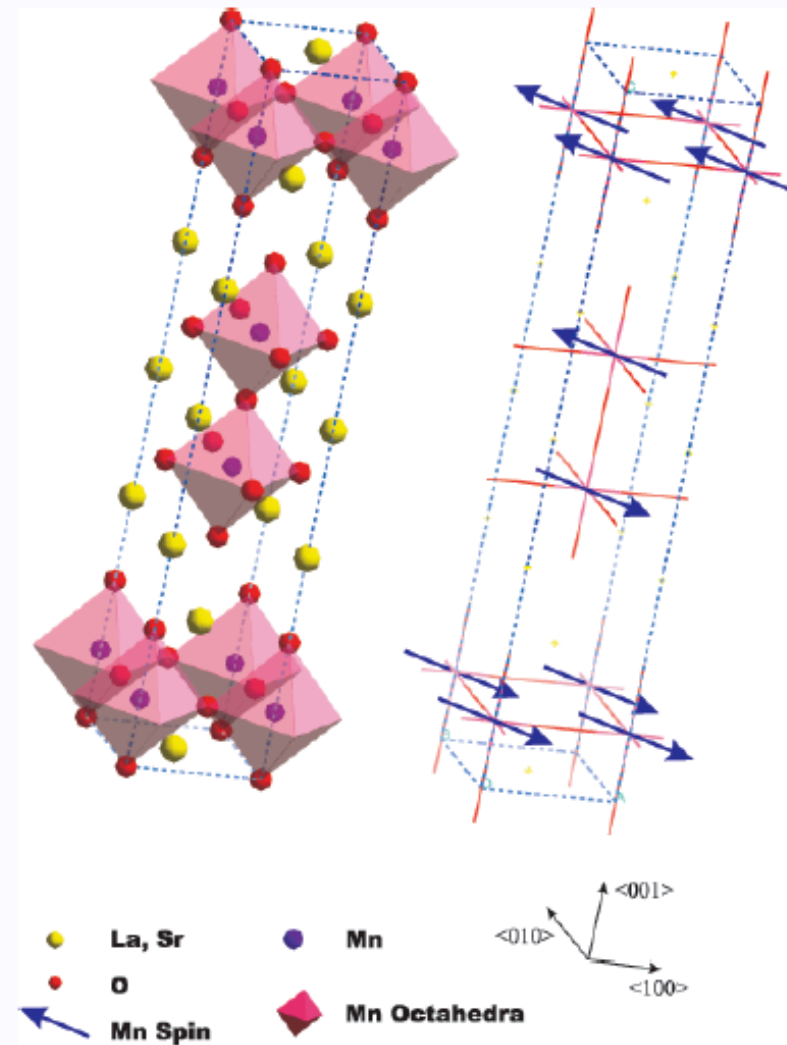
(Received 28 January 2003; published 8 May 2003)

We have conducted the first soft x-ray diffraction experiments from a bulk single crystal, studying the bilayer manganite $\text{La}_{2-2x}\text{Sr}_{1+2x}\text{Mn}_2\text{O}_7$ with $x = 0.475$ in which we were able to access the (002) Bragg reflection using soft x rays. The Bragg reflection displays a strong resonant enhancement at the L_{III} and L_{II} manganese absorption edges. We demonstrate that the resonant enhancement of the magnetic diffraction of the (001) is extremely large, indeed so large that it exceeds that of the nonresonant Bragg diffraction. Resonant soft x-ray scattering of 3d transition metal oxides is the only technique for the atomic selective measurement of spin, charge, and orbital correlations in materials, such as high temperature superconductors, colossal magnetoresistance manganites, and charge stripe nickelates.

Spin ordering in $\text{La}_{2-2x}\text{Sr}_{1+2x}\text{Mn}_2\text{O}_7$

Two dimensional layered structure

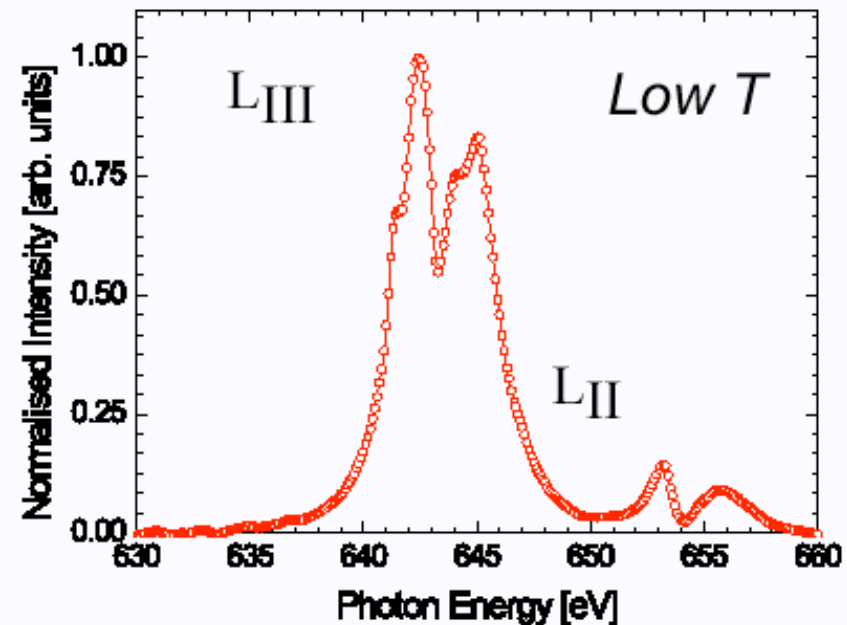
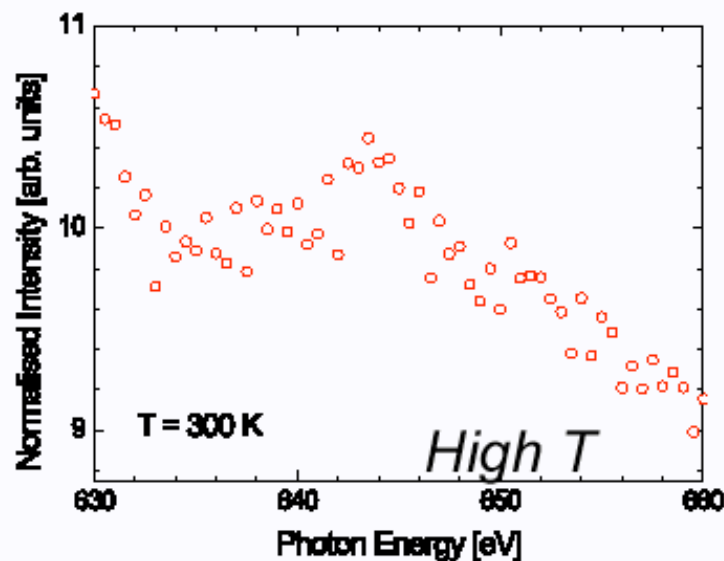
*At low temperatures
the Mn^{3+} and Mn^{4+}
ions spin order
antiferromagnetically*



Resonant magnetic exchange scattering

Below T_N the (001) is resonantly enhanced at the L_{III} and L_{II} edges

$2p \Rightarrow 3d$ transition



Above T_N only weak charge scatter is observed – no resonance. The (001) is due to AFM magnetic scattering.